Model-Free Control for Tidal Current Turbine Generation Systems: A Comparative Study

Zhibin Zhou, Jean-Matthieu Bourgeot, Yassine Amirat, Mohamed Benbouzid

Model-Free Control for Tidal Current Turbine Generation Systems: A Comparative Study

Zhibin Zhou[1], Jean-Matthieu Bourgeot[2], Yassine Amirat[1], Mohamed Benbouzid[3,4]
[1]L@bISEN, ISEN Yncréa Ouest, Brest, France
[2]ENIB, UMR CNRS 6027 IRDL, Brest, France
[3]University of Brest, UMR CNRS 6027 IRDL, Brest, France
[4]Shanghai Maritime University, Shanghai, China
Email: zhibin.zhou@isen-ouest.yncrea.fr, bourgeot@enib.fr,
yassine.amirat@isen-ouest.yncrea.fr, Mohamed.Benbouzid@univ-brest.fr

***Abstract* — During recent years, tidal current turbine systems have been exploited as a promising technology of generating electricity from the sea tides. Traditional PI control may suffer from unpredictable distances or parameter uncertainties. More advanced control strategies such as sliding mode control (SM), active disturbance rejection control (ADRC), and model-free control (MFC) should be applied for improving the system performance. The objective of this work is to carry out a comparative study for the four control strategies. The control structure and the characteristics will be presented for each control strategy, and then controllers based on different strategies are applied in the turbine-generator speed loop to verify the generation system performance under water flow speed changes and turbine torque disturbances. From the simulation comparisons, the ADRC control and MFC based intelligent proportional (iP) controller showed better performance in terms of tracking speed and smooth response under various conditions.**

***Keywords* — Tidal turbine generation, disturbance rejection control, sliding mode control, model free control.**

I. INTRODUCTION

Following the wind turbine technologies, the development to harness kinetic energy from tidal current is very fast during the last 20 years, different tidal current turbine projects have been tested in the real sea environments [1-2]. These projects showed us a promising future of supplying electricity for some islands and coastal areas. Challenges such as marine current speed variations and unpredictable disturbances can deteriorate the performance of turbine-generation systems. Therefore, it is interesting to compare different control strategies for the turbine-generator system under these challenges. In [3-4], active disturbance rejection control (ADRC) strategy is proposed and compared with PI and sliding mode (SM) controls to show its effectiveness. This paper will include the model-free control (MFC) based intelligent proportional (iP) controller in the comparative study to give an insight for choosing the appropriate control strategy for turbine-generation applications.

For a turbine with non-pitchable blades, the power coefficient (C_p) of the turbine will mainly depend on the tip speed ratio (TSR). A speed control or torque control in the turbine-generation system is therefore necessary to generate maximum power from varying tidal currents [5]. PID control strategy is widely applied in industrial applications due to simple structure and relative easy parameter tuning, but it presents several drawbacks such as: 1) sensitivity to the noise; 2) overshoot or saturation caused by the integration term; 3) accurate plant model is usually needed for calculating the controller gains. In fact, some plant parameters may be unavailable or present variable values under different operation conditions. These drawbacks can be partially avoided by using modified PID-based methods or sliding mode control strategies [6-8], and other controller designs such as ADRC and MFC can be more efficient due to their less dependence on the plant parameters and better disturbance rejection [9-12]. In an ADRC strategy, all types of varying dynamics or unknown plant parameters are generalized as a "total disturbance" which is estimated through a state observer and then compensated in the controller output. A linear ADRC (LADRC) can have simple rules for parameters tuning but a non-linear control law of ADRC may benefit an advantage of not needing accurate plant parameters. In a MFC strategy, the unknown parts of the plant and various possible disturbances are also continuously estimated by a filter-based function.

In this paper, four control strategies: classical PI, non-linear ADRC, second-order SM and MFC are applied on a permanent magnet synchronous generator (PMSG) based turbine-generation system under disturbances. Their performances are compared and analyzed. In Section II, the controller structures and parameter settings based on four different control strategies for the turbine-generator system speed control are presented. In Section III, the simulation results of the four strategies under sudden water flow speed change and turbine torque disturbance are compared. The energy production during swell wave variations are also compared.

II. TURBINE-GENERATOR SYSTEM AND CONTROLS

Similar to a wind turbine, the mechanical power harnessed by a tidal stream turbine is expressed by

$$P = \frac{1}{2}\rho C_p(\lambda)\pi R^2 V_{tide}^3 \tag{1}$$

where, ρ is the seawater density and R is the turbine radius; V_{tide} is the velocity of tidal stream; C_p is the turbine power coefficient. From the hydrodynamics of the turbine, the C_p values can be calculated by a function of the pitch angle and

the tip speed ratio (TSR) λ. A non-pitchable turbine is considered and the C_p - λ characteristics are shown in Figure 1. The maximum C_p value can be obtained when λ_{opt} = 6.3; and this optimal tip speed ratio should be maintained via the controller for operating the turbine-generation system at its maximum power coefficient.

The maximum power point tracking (MPPT) can be realized by adjusting the turbine-generator rotational speed according to the tidal water flow speed, thus the system can always operate at its optimal λ_{opt} and maximum C_p. If there is a gearbox connecting the turbine and the generator rotor (with a speed ratio G_g), then the generator speed reference can be calculated by

$$\omega_m^* = G_g \cdot \frac{\lambda_{opt} V_{tide}}{R} \tag{2}$$

The model for the PMSG is given by the following equations

$$\begin{cases} v_d = R_s i_d + L_d \dfrac{\mathrm{d}i_d}{\mathrm{dt}} - \omega_e L_q i_q \\ v_q = R_s i_q + L_q \dfrac{\mathrm{d}i_q}{\mathrm{dt}} + \omega_e L_d i_d + \omega_e \psi_m \\ T_e = \dfrac{3}{2} n_p \left[\psi_m i_q + (L_d - L_q) i_d i_q \right] \\ J \dfrac{\mathrm{d}\omega_m}{\mathrm{dt}} = T_m - T_e - f_B \omega_m \end{cases} \tag{3}$$

where, v_d, v_q and i_d, i_q are respectively stator voltages and currents in the d-q axis; R_s is the stator resistance; L_d, L_q are inductances in the d-q axis ($L_d = L_q = L_s$ for the non-salient machine considered in this study); ω_e, ω_m are electrical and mechanical angular speed; T_e and T_m represent the electromagnetic torque and the mechanical torque; n_p is the generator pole pair number; ψ_m is the PM rotor flux linkage; J is the total system inertia and f_B is the friction coefficient of the drive train.

Figure 2 shows the turbine-generation system control diagram. This study focuses on different strategies for the speed controller. The current controllers are based on PI control and will not change while comparing different speed controllers.

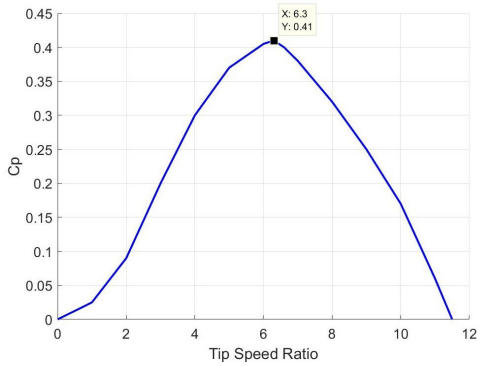

Fig. 1. C_p -λ characteristic of the turbine.

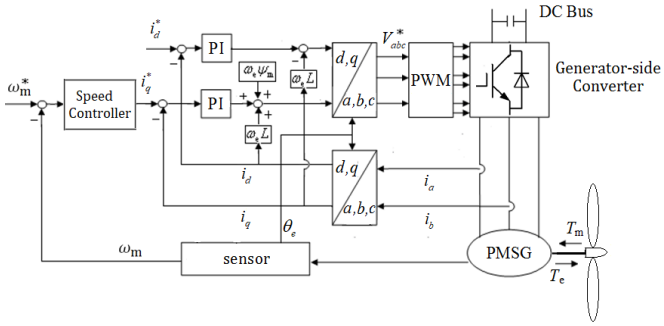

Fig. 2. Speed and current control loops for the studied system.

A. Classical PI Control

The PI current controllers are tuned before the speed controller. The two PI current controllers can share same parameters due to the similar dynamics of i_d and i_q loops. The open-loop transfer function of the PI controller based current loop can be expressed as:

$$G_0(s) = \frac{K_p(\tau_i s + 1)}{\tau_i s} \cdot \frac{1/R_s}{\left[(L_s/R_s)s + 1\right](T_{\Sigma i} s + 1)} \tag{4}$$

with K_p and $K_i = 1/\tau_i$ as controller parameters and $T_{\Sigma i}$ (smaller than the electrical time constant L_s/R_s) represents the delays in the current loop. By using the dominant pole cancelation method and with a desired damping factor (0.707 in our case) for the close-loop transfer function, the PI current controller parameters can be set by

$$\begin{cases} K_i = R_s / L_s \\ K_p = R_s \big/ \left(2 T_{\Sigma i} K_i\right) \end{cases} \tag{5}$$

From Figure 2, the speed controller is to generate the q-axis current reference i_q^*. The d-axis current reference i_d^* is set to 0 for maximizing the electromagnetic torque. The non-symmetrical optimum method (NSOM) is applied to tune the PI speed controller. The NSOM utilizes a second-order approximated model of the plant with a generalized time constant ($T_Q = 1/\omega_Q$), and K_Q which can be obtained from slope rate of open-loop step response. Then, the PI speed controller can be obtained by:

$$\begin{cases} K_{ps} = \gamma_c \dfrac{\omega_Q}{K_Q \sqrt{\alpha_c}} \\ K_{is} = \dfrac{\omega_Q}{\alpha_c} \end{cases} \tag{6}$$

where, γ_c is based on the desired resonant peak value M_c and the α_c is calculated by the phase advance which is related to γ_c. Details of the NSOM tuning are presented in [13-14].

Based on the presented methods, the PI current controllers are tuned as K_p = 6.5 and K_i = 100; and the parameters of the PI speed controller are set as K_{ps} = 1.3 and K_{is} = 4.9.

B. ADRC Strategy

This strategy utilizes a non-linear control (NLC) law and an extended state observer (ESO) to obtain quick tracking speed and efficient disturbance rejection. The plant should be firstly expressed by a canonical state-space form, and then all disturbances and unknown plant dynamics are modeled as an extended state variable [15]. The first-order derivation of the controlled variable *y* can be modeled as

$$\begin{cases} \dot{x}_1 = F + b \cdot u \\ y = x_1 \end{cases} \tag{7}$$

where, u is the plant input, b is a system constant, and F models the generalized disturbance (including all unknown dynamics and disturbances). In fact, F will be considered as an extended state variable to be estimated by the observer. Figure 3 shows the controller structure, where e represents the input error signal; b_0 represents an approximate value of the constant b described in (7); and the observer ESO generates two outputs: z_1 is an estimation of the plant output and z_2 is the estimated generalized disturbance.

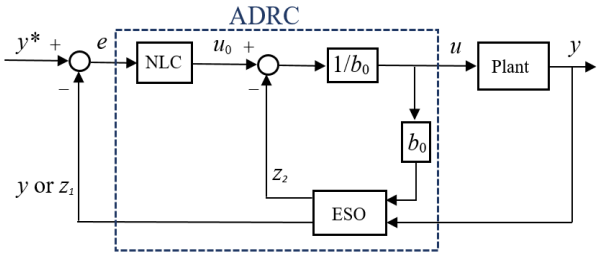

Fig. 3. Control structure of ADRC.

In our case, the variable to be controlled is the generator rotor speed $y = \omega_m$, and the controller output will be the q-axis current reference $u = i_q^*$. Then, the first-order generator rotor speed can be expressed by

$$\dot{\omega}_m = \left(-\frac{T_m}{J} - \frac{f_B \omega_m}{J}\right) + \frac{1.5 n_p \psi_m}{J} i_q^* \tag{8}$$

It should be noted that all unknown disturbances and variations of the plant parameters (T_m, f_B, ω_m and J) will be generalized as the total disturbance F and estimated by the ESO.

The non-linear function called *fal* is applied in the ADRC as proposed in [9],

$$fal(x,\alpha,\delta) = \begin{cases} |x|^{\alpha} \operatorname{sign}(x), & |x| > \delta \\ \dfrac{x}{\delta^{1-\alpha}}, & |x| < \delta \end{cases} \tag{9}$$

with x as the main input representing error information; $0 < \alpha < 1$ makes the function to have a reducing effect with large x input and to avoid saturation; and $\delta > 0$ gives a linear zone for avoiding too large output value when the error signal x is small enough around 0. Based on this non-linear function, the NLC output can then be given by $u_0 = k_1 \cdot fal(e, \alpha_0, \delta)$.

The ESO is constructed as

$$\begin{cases} \varepsilon = z_1 - y = z_1 - \omega_m \\ \dot{z}_1 = z_2 + b_0 u - \beta_1 \cdot fal(\varepsilon, \alpha_1, \delta) \\ \dot{z}_2 = -\beta_2 \cdot fal(\varepsilon, \alpha_2, \delta) \end{cases} \tag{10}$$

And the ADRC speed controller output is calculated by

$$u = i_q^* = \left(k_1 \cdot fal(e, \alpha_0, \delta) - z_2\right) / b_0 \tag{11}$$

The observer gains β_1, β_2 and the controller gain k_1 are tuned by simulations and set with values of $\beta_2 = 100$, $\beta_1 = 120$, $k_1 = 350$; and other parameters are set as $\delta = 0.1$, $\alpha_0 = 0.3$, $\alpha_1 = 0.5$ and $\alpha_2 = 0.25$.

C. SM Control Strategy

Sliding mode is another interesting non-linear robust control method for systems presenting non-linear dynamics and parameter variations [16-17]. For the turbine-generator speed controller, the sliding surface can be defined by the speed tracking error

$$s_1 = \omega_m^* - \omega_m \tag{12}$$

and the super-twisting SM control law can be applied as following equation

$$u = i_q^* = K_1 \cdot |s_1|^{0.5} \operatorname{sign}(s_1) + K_2 \int \operatorname{sign}(s_1) \tag{13}$$

The controller gains K_1 and K_2 could be tuned by trial and error method via simulations, and $K_1 = 3$ and $K_2 = 30$ are chosen in this work for good tracking performance and low output chattering.

D. MFC Strategy

Model-free control is based on the fact that during very small-time interval, the system (and all its complexity and non-linearity) can be presented by a purely numerical model with one input *(x)* and one output *(y)* as a SISO system, and F represents all the unknown system dynamics [12].

For this application, a first order purely numerical model is considered to represent the local system

$$\dot{y} = F + \alpha \cdot u \tag{14}$$

Measurement of y and knowledge of u are used to compute an estimation of the unknown dynamics, noted as $[F]_e$. This estimation is done at each step by

$$[F]_e = [\dot{y}] - \alpha \cdot u \tag{15}$$

where $[\dot{y}]_e$ is an estimation of $\dot{y}$ from only measurement of y and the last value of the input u. The controller is performed by using the 'intelligent PID" law given by

$$u = \frac{1}{\alpha}\left(-[F]_e + \dot{y}^* - k_p e - k_I \int e - k_D \dot{e}\right) \quad (16)$$

with $e = y - \dot{y}$ is the error information.

In this work, $k_I = 0$ and $k_D = 0$, then the resulted MFC controller becomes an intelligent proportional (iP) controller and the dynamic of the error is reduced to $\dot{e} + k_P e = 0$. In this way, the convergence speed of error elimination can be tuned by k_P. The major benefit of MFC is that the tuning of gain becomes very simple. In the following simulation, the gains are chosen as $k_P = 200$ and $\alpha = 750$.

For the notations in our application, the MFC speed controller output u represents i_q^* and the plant output y represents the generator rotational speed ω_m. The application of the control law can be re-written as

$$u = i_q^* = \frac{1}{\alpha}\left(-[F]_e + \dot{\omega}_m^* - k_p\left(\omega_m - \omega_m^*\right)\right) \quad (17)$$

It should be noted that the derivative terms $\dot{y}$ and $\dot{y}^*$ are not directly available from the sensors, but they can be obtained from algebraic derivative estimators [18-19]. A finite impulse response (FIR) filter implementation of the derivative estimators is used as in [20]. The time step of the control law is set to $T_s = 0.1$ ms, and the sampling time of the simulation (the time step of the acquisition of ω_m) is set to 0.01 ms ; indeed 10 points are necessary for the FIR filter to obtain a good estimation of the derivative term.

III. Simulation Results

A laboratory-scaled PMSM is studied in the simulation. The constants of the studied turbine-generator system are listed in Appendix. In the flowing part, system performances under a sudden tidal current velocity change and a turbine torque disturbance are presented; and then, the tracking performance and energy production under varying tidal current are compared by applying the four different speed controllers.

A. Sudden Changes of Water Flow Speed and Torque

The water flow speed without disturbances is set as a constant 2 m/s during the simulation. A sudden water flow speed reduction (-0.7 m/s as the peak) is applied during 6 s and 6.6 s, and a large turbine torque disturbance of 12 Nm is added from 11s to 11.5 s.

With gearbox speed ratio $G_g = 3.544$, turbine blade radius R = 0.32 m, and λ_{opt} = 6.3, the generator rotor speed should follow the speed reference of 139.5 rad/s, as calculated by (2) at steady-state.

The rotor speed responses of the generator at the beginning stage under different speed control strategies are illustrated by Figure 4. It shows that the PI controller produces an overshoot of 7.4 rad/s (5.3% of the steady-state speed), and it takes more time for reaching the steady-state speed. Compared by the PI controller, the SM controller has a smaller overshoot about 3% with a shorter convergence time. The MFC and ADRC controllers show the best performance; they use the shortest time for convergence and they present no visible overshoot. Table 1 summarizes the speed tracking performance during the starting stage

Table 1. Performance during the starting stage

	Overshoot (%)	Settle Time (s)
PI	5.3	0.7
SM	3	0.4
ADRC	0.3	0.2
MFC	0	0.2

During the sudden marine current speed drop between 6 s and 6.6 s, all the four controllers are capable of following a dropping speed reference as illustrated by Figure 5.

When the water flow disturbance is cleared (6.6 s), the speed reference has a step rise. In this case, a rapid acceleration is required for the generator-turbine system to reach the speed before the disturbance. This acceleration process is quite similar to the starting stage and it can be seen that SM, ADRC and MFC show better speed tracking than the PI controller.

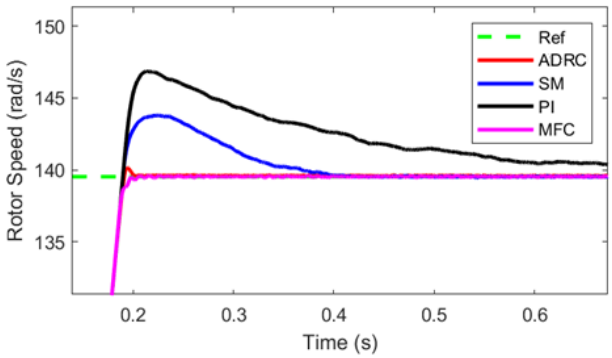

Fig. 4. Generator speed during the starting stage.

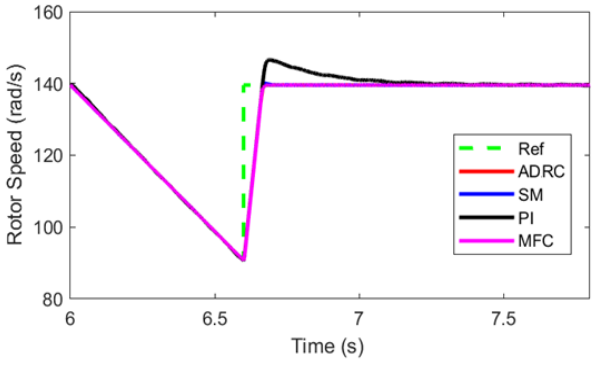

Fig. 5. Speed tracking during sudden water flow change.

During the period from 11 s to 11.5 s, an extra mechanical torque (12 Nm) is applied to simulate a sudden disturbance on the turbine blades. Figure 6 shows the generator speed variations under the instant torque disturbance. We can see that the torque disturbance at 11 s causes a generator speed increase and the clearance of the disturbance at 11.5 s leads to a speed fall by the PI speed controller. The SM controller can reduce the tracking error with shorter time. The MFC achieves the smallest maximum tracking error and both ADRC and MFC present no speed drop error after 11.5 s when the torque disturbance disappears. The generator power peaks caused by the torque disturbance are shown by Figure 7. The ADRC and MFC demonstrate smooth responses and good disturbance rejection.

Table 2. Performance during the torque disturbance

	Maximum Speed Error (%)	Resulted Power Peak (W)
PI	3.5	2240
SM	2.4	2230
ADRC	1.5	2225
MFC	0.8	2220

B. Energy Production under Varying Current Speed

Swell waves are the main cause of tidal water flow speed fluctuations for tidal current turbine systems. Figure 8 shows the marine current fluctuations under swell effect in the simulation.

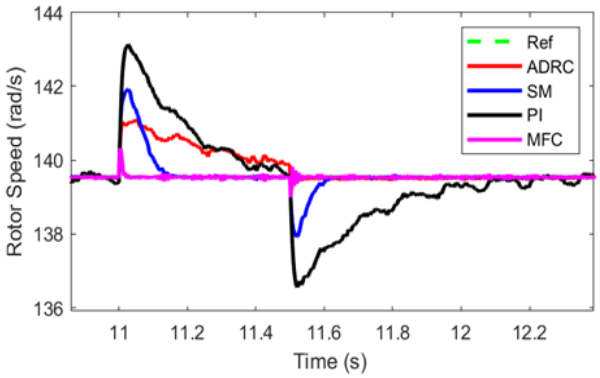

Fig. 6. Speed tracking under torque disturbance.

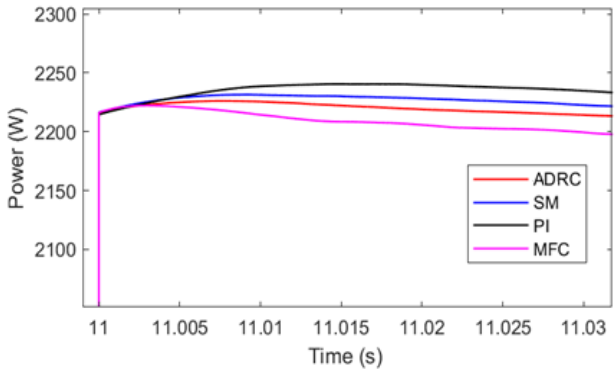

Fig. 7. Peak power of the generator under torque disturbance.

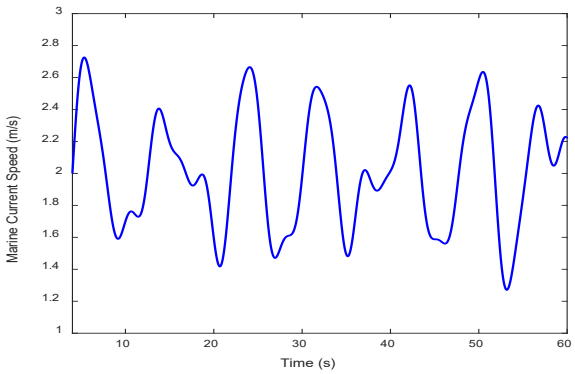

Fig. 8. Varying marine current speed.

In this case, under varying marine current speed, the generator speed tracking performances and the produced energies under the studied strategies are quite close. Each speed controller studied in this work can successfully keep the turbine-generator system following the speed reference with very small tracking errors.

Figure 9 illustrates the speed tracking errors for the four studied control strategies. It can be observed that ADRC, SM and MFC speed controllers are capable of limiting the tracking errors between -0.1 rad/s and +0.1 rad/s under the varying marine current speed; and the PI speed controller leads to a tracking errors range between -0.3 rad/s and +0.3 rad/s.

The energies produced by the turbine-generator system during the varying current period are shown in Figure 10. It can be seen that the energy production by applying the PI speed control strategy is about 31.875 kJ; SM and MFC lead to the same energy yielding with 31.887 kJ and ADRC can produce 31.888 kJ at the end of simulation (60 s).

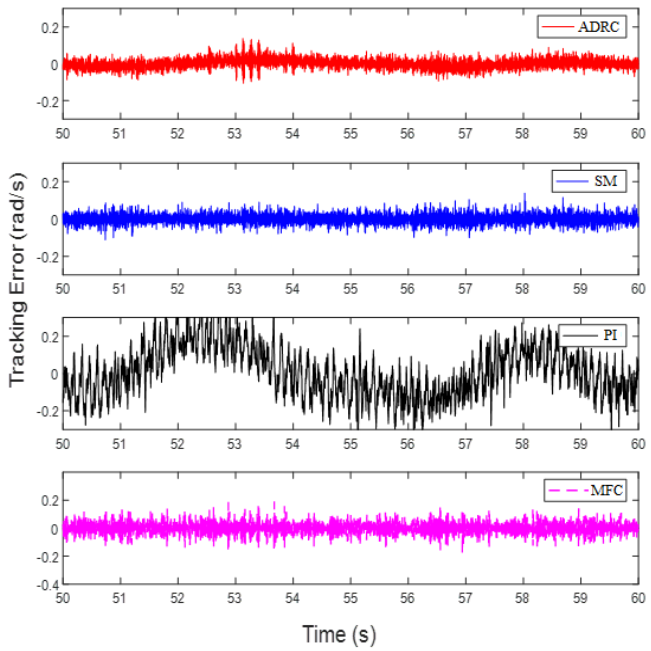

Fig. 9. Generator speed tracking error under varying marine current velocity.

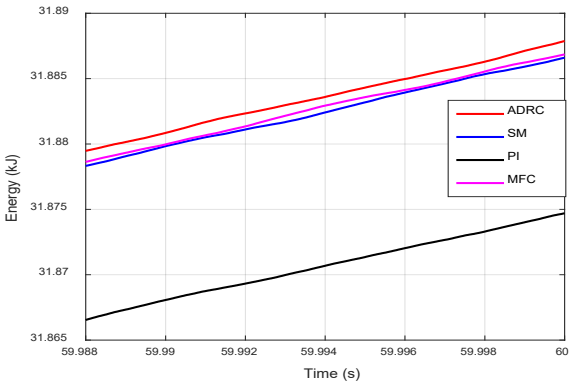

Fig. 10. Generator produced energies by different speed controllers.

IV. Conclusion

The four control strategies: PI control, active disturbance rejection control, sliding mode control and model-free control are applied for the PMSG-based tidal stream turbine system to compare their speed tracking performances. The classical PI controller and the super-twisting based sliding mode controller benefit from simple control structure and they are easy to apply with less controller parameters. ADRC and MFC have more powerful disturbance rejection capabilities because both strategies enable to compensate unknown disturbances by implement of an observer/estimator in their control algorithms. The simulation results demonstrate that ADRC and MFC have best performance during sudden current velocity and torque disturbances. The energy production results show that ADRC, MFC and SM have similar performances and they are much better than the classical PI control strategy.

Appendix

Parameters of the Turbine-Generator System

Blade radius of the turbine	0.32 m
Maximum C_p	0.41
Optimal tip speed ratio for MPPT	6.3
Nominal marine current speed	3.0 m/s
Total system inertia	0.03 kg$\cdot$m^2
Friction coefficient	0.0035
Generator nominal power	1.82 kW
Generator nominal torque	8.7 Nm
DC-bus voltage	700 V
Generator nominal speed	209.4 rad/s
Gearbox speed ratio	3.544
Generator pole pair number	3
Rotor permanent magnet flux	0.5333 Wb
Stator resistance	1.3 Ω
d-q axis stator inductances	13 mH

References

[1] Z. Zhou, M.E.H. Benbouzid, J.F. Charpentier, F. Scuiller and T. Tang, "Developments in large marine current turbine technologies - a review," *Renewable and Sustainable Energy Reviews*, vol. 77, pp. 852-858, May 2017.

[2] H. Chen, T. Tang, N. Aït-Ahmed, M. E. H. Benbouzid, M. Machmoum and M. E. Zaïm, "Attraction, Challenge and Current Status of Marine Current Energy," *IEEE Access*, vol. 6, pp. 12665-12685, 2018.

[3] Z. Zhou, S. Benelghali, M. Benbouzid, Y. Amirat, E. Elbouchikhi, G. Feld, "Tidal stream turbine control: An active disturbance rejection control approach," *Ocean Engineering*, vol. 202, 107190, pp. 1-9, march 2020.

[4] Z. Zhou, S. Benelghali, M.E.H. Benbouzid, Y. Amirat, E. Elbouchikhi and G. Feld, "Control strategies for tidal stream turbine systems – a comparative study of ADRC, PI, and High-order sliding mode controls," in *Proceedings of the 45the IEEE Conference of the Industrial Electronics Society*, Lisbon (Portugal), pp. 6981-6986, October 2019.

[5] Z. Qin, X. Tang, Y. Wu and S. Lyu, "Advancement of tidal current generation technology in recent years: a review," *Energies*, vol. 15, 8042, pp.1-18, 2022.

[6] H. Benbouhenni, N. Bizon, I. Colak, P. Thounthong and N. Takorabet, "Application of fractional-order PI controllers and neuro-fuzzy PWM technique to multi-rotor wind turbine systems," *Electronics*, vol. 11, 1340, pp.1-26, 2022.

[7] Y. Belkhier, A. Achour, N. Ullah, R.N. Shaw, Z. Farooq, et al. "Intelligent energy-based modified super twisting algorithm and factional order PID control for performance improvement of PMSG dedicated to tidal power system," *IEEE Access*, vol. 9, pp. 57414-57452, 2021.

[8] O. Rodriguez-Abreo, J. Rodriguez-Resendiz, C. Fuentes-Silva, R. Hernandez-Alvarado and M. Falcon, "Self-tuning neural network PID with dynamic response control," *IEEE Access*, vol. 9, pp. 65206-65215, 2021.

[9] J. Han, "From PID to active disturbance rejection control," *IEEE Transactions on Industrial Electronics*, vol. 56, n°3, pp. 900-906, March 2009.

[10] Y. Huang, W. Xue, G. Zhiqiang, H. Sira-Ramirez, D. Wu and M. Sun, "Active disturbance rejection control: Methodology, practice and analysis," in *Proceedings of the 33rd Chinese Control Conference*, Nanjing (China), pp. 1-5, July 2014.

[11] Z. Shi, P. Zhang, J. Lin and H. Ding, "Permanent magnet synchronous motor speed control based on improved active disturbance rejection control," Actuators, vol. 10, 147, pp.1-16, 2021.

[12] M. Fliess and C. Join, "Model-free control," *International Journal of Control*, vol. 86, n°12, pp. 2228-2232, Jul. 2013.

[13] Z. Zhou, "Modeling and power control of a marine current turbine system with energy storage devices," PhD thesis, University of Brest (France), pp. 43-47, Oct. 2014.

[14] T. Ane and L. Loron, "Easy and efficient tuning of PI controllers for electrical drives," in *Proceedings of the 2006 IEEE IECON*, Paris (France), pp.5131-5136, Nov. 2006.

[15] B. Guo, S. Bacha and M. Alamir, "A review on ADRC based PMSM control designs," in *Porceedings of the 2017 IEEE IECON*, Beijing (China), pp. 1747-1753, Oct. 2017.

[16] S. Benelghali, M. E. H. Benbouzid, J. F. Charpentier, et al., "Experimental validation of a marine current turbine simulator: application to a permanent magnet synchronous generator-based system second-order sliding mode control," *IEEE Transactions on Industrial Electronics*, vol. 58, n°1, pp. 118-126, Jan. 2011.

[17] D.H. Phan and S. Huang, "Super-twisting sliding mode control design for cascaded control system of PMSG wind turbine," *Journal of Power Electronics*, Vol. 15, n°5, pp. 1358-1366, Sept. 2015.

[18] M. Fliess and H. Sira-Ramrez, "An algebraic framework for linear identication," *ESAIM Control Optimiz. Calc. Variat.*, vol. 9, pp. 151–168, Sep. 2003.

[19] M. Mboup, C. Join and M. Fliess. "A revised look at numerical differentiation with an application to nonlinear feedback control," in *Proceedings of the 15th Mediterranean Conference on Control and Automation*, Athenes (Greece), June 2007.

[20] P.A. Gédouin, E. Delaleau, J.M. Bourgeot, C. Join, S. Arbab Chirani and S. Calloch, "Experimental comparison of classical PID and model-free control: Position control of a shape memory alloy active spring," *Control Engineering Practice*, Vol. 19, n°5, pp. 433-441, 2011.